Applied Food Research 6 (2026) 102818

Contents lists available at ScienceDirect

Applied Food Research

journal homepage: www.elsevier.com/locate/afres

Dechlorophyllized ethanolic extract of kenikir (*Cosmos caudatus*) leaf: Antioxidant activities and its effect on properties and oxidative stability of sardine surimi gel

Muh Ali Arsyad [a], Natchaphol Buamard [b], Mallikarjun Chanchi Prashanthkumar [c], Umesh Patil [b], Soottawat Benjakul [b,*]

[a] *Department of Agricultural Technology, Pangkep State Polytechnic of Agriculture, South Sulawesi, Indonesia*
[b] *International Center of Excellence in Seafood Science and Innovation (ICE-SSI), Faculty of Agro-Industry, Prince of Songkla University, Hat Yai, Songkhla, 90110, Thailand*
[c] *Faculty of Agricultural Technology, Songkhla Rajabhat University, Khao-Rupchang, Muang, Songkhla, 90000, Thailand*

ARTICLE INFO

Keywords:
Cosmos caudatus
Dechlorophyllization
Kenikir leaf extract
Surimi gel
Phenolic–protein interactions
Oxidative stability
Clean-label additive

ABSTRACT

Dechlorophyllized ethanolic kenikir (*Cosmos caudatus*) leaf extract (KLE-D) was prepared as a natural functional additive. Dechlorophyllization via sedimentation effectively reduced chlorophyll content while maintaining a comparable total phenolic concentration. DPPH radical-scavenging activity increased after dechlorophyllization, whereas ABTS radical-scavenging activity, FRAP, and metal-chelating activity remained unchanged. Based on LC-QTOF-MS/MS analysis, KLE-D contained 24 putatively identified compounds. The incorporation of KLE-D into sardine surimi gels influenced gel properties. The addition of 0.1% KLE-D yielded the strongest gel, as evidenced by the highest breaking force, deformation, hardness, gumminess and chewiness along with the lowest expressible moisture content. KLE-D addition also enhanced elastic modulus (G′) in surimi paste during thermal gelation. Rheological measurements and gel microstructure observations supported the enhancement of gel strength. Although the underlying chemical interactions were not clearly identified, these results implied that KLE-D could strengthen the gel networks. In contrast, an excessive KLE-D addition (0.125%) disrupted network uniformity and lowered gel quality. During 8 days of refrigerated storage, surimi gels containing 0.1% KLE-D exhibited significantly lower lipid oxidation as indicated by the lower increases in PV and TBARS value. Overall, KLE-D at an optimal concentration (0.1%) functioned as an effective clean-label additive that enhanced gel strength and oxidative stability in surimi gels.

1. Introduction

Surimi, a proteinaceous concentrate obtained mainly from fish myofibrillar proteins, is an important ingredient in the production of gel-based seafood products, such as fish balls, crab sticks, kamaboko, etc. (Yang et al., 2025). Due to its ability to produce heat-induced gels with excellent textural properties, surimi is considered a basic ingredient in the seafood processing industry (Xie et al., 2024). Nevertheless, the surimi produced from most dark-fleshed species like sardine yields the poor gel, mainly because of excessive endogenous proteases, susceptibility to lipid oxidation, and low gel-forming ability (G. Han & Li, 2024). These inherent shortcomings have led to the search for natural bioactive compounds as potential additives to improve surimi gelling properties and storage stability.

Plant extracts rich in polyphenols have received widespread attention in recent years as clean-label substitutes for synthetic additives. Apart from their strong antioxidant potential, polyphenolic compounds can be used for inducing protein cross-linking via hydrogen bonds, hydrophobic interactions, and covalent bonds (Arsyad et al., 2018). These interactions have been shown to strengthen the gel matrix with enhanced water holding ability. Ethanolic extracts from duea ching (Buamard et al., 2024), coconut husk (Buamard et al., 2017), lotus root (X. Han et al., 2024), fig (*Ficus botryocarpa*) (Ayuso et al., 2022), and citrus peels (Fathy et al., 2022) have been documented to strengthen surimi gel. Kenikir (*Cosmos caudatus*) is a commonly consumed traditional leafy vegetable in Southeast Asia that is rich in flavonoids and

* Corresponding author.
E-mail address: soottawat.b@psu.ac.th (S. Benjakul).

https://doi.org/10.1016/j.afres.2026.102818
Received 23 September 2026; Received in revised form 21 October 2026; Accepted 4 November 2026
Available online 5 November 2026
2772-5022/© 2026 The Authors. Published by Elsevier B.V. This is an open access article under the CC BY-NC license (http://creativecommons.org/licenses/by-nc/4.0/).

phenolic acids with potential multifunctional roles (Abidin et al., 2025). Kenikir leaves are known to contain a natural pigment called chlorophyll. This pigment contributes to the greenish color of the resulting extract. Due to this natural green coloring, kenikir leaf extract may have limitations when applied to foods that require a typical color. One way to remove chlorophyll from plant extracts is through sedimentation (Singh et al., 2023; Tagrida & Benjakul, 2020). Although sedimentation removes chlorophyll, it may also change the chemical composition and functional capabilities of the final product . Alternatively, undesirable pigment can be removed via this process without destroying active compounds associated with kenikir leaf extract. Kenikir (*Cosmos caudatus*) is a common plant, and its polyphenol-rich extract could enhance the quality of surimi gels and prevent oxidation. Surimi produced from sardine, a dark-fleshed fish and may have difficulty forming good gels, as well as being highly susceptible to lipid oxidation (Panpipat et al., 2023). Therefore, plant-derived extracts rich in polyphenols have the potential to enhance gel characteristics, and reduce lipid oxidation in the product during refrigerated storage. However, no study on the application of dechlorophyllized ethanolic kenikir leaf extract (KLE-D) in sardine surimi gel exists. Therefore, the effect of dechlorophyllization on the extract composition and antioxidant activity was studied. The impact of the addition of KLE-D on the properties of sardine surimi gel and lipid oxidation of surimi gel during refrigerated storage was also investigated. The dechlorophyllized kenikir leaf extract could serve as a novel multifunctional additive for sardine surimi gel.

2. Materials and methods

2.1. Preparation of ethanolic kenikir leaf extract (KLE)

The powdered leaf of kenikir was purchased from Rempah Bu Risma, Bekasi, Indonesia. The ethanolic kenikir leaf extract was prepared according to the method described by Cava and Ladero (2024). The ratio of leaf powder to the solvent (70% ethanol) was 1:10 (w/v) (Raspe et al., 2022). Extraction was carried out at 25 °C for 120 min under constant agitation with a magnetic stirrer. The samples were centrifuged at 5,000 × g for 5 min, then passed through Whatman® No. 4 qualitative filter paper. Ethanol was removed from the extract at 40 °C using a Büchi rotary evaporator (B-100, PT. Büchi, Jakarta, Indonesia). The remaining ethanol was removed by nitrogen flushing.

The extraction yield was calculated based on the dry mass of the ethanolic extract relative to the initial mass of kenikir leaf powder. Extraction yield was reported as the percentage (Latiff et al., 2021; Moshawih et al., 2017).

2.2. Chlorophyll removal of ethanolic extract

Chlorophyll was removed from the ethanolic extract by sedimentation method (Ahmad et al., 2024). After ethanol was evaporated, the extract was diluted with distilled water at a 1:1 (v/v) ratio and allowed to stand at 4 °C for 24 h for sedimentation, after which the upper fraction was collected and the sediment was discarded. The collected top fraction was centrifuged (4,000 × g for 30 minat 4 °C). The resulting supernatant was frozen at −20 °C prior to lyophilization (Scanvac Coolsafe 55, Coolsafe, Lynge, Denmark). The dechlorophyllized ethanolic extract powder was named 'KLE-D', while an ethanolic extract powder without chlorophyll removal was referred to as KLE. The extract powders with and without dechlorophyllization were then analyzed.

The solid recovery following dechlorophyllization was calculated as the mass of dried KLE-D recovered after dechlorophyllization divided by the initial dry mass of KLE. The recovery was expressed as the percentage.

2.3. Characterization of KLE and KLE-D

2.3.1. Total phenolic content (TPC)

Total phenolic contents (TPC) of KLE and KLE-D were analyzed employing the Folin–Ciocalteu assay (Mittal et al., 2022). TPC was expressed as milligrams of gallic acid equivalents (GAE) per gram of dry extract. The total phenolic recovery following dechlorophyllization was determined and divided by the TPC concentration found in KLE. The recovery was reported as the percentage.

2.3.2. Chlorophyll content

Chlorophyll content of KLE and KLE-D was determined spectrophotometrically. Total chlorophyll, chlorophyll a and chlorophyll b contents were examined (Olatunde et al., 2018).

2.3.3. Antioxidant activities

Antioxidant activities of both extract powders were determined using several assays including DPPH radical scavenging activity (D-RA), ABTS radical scavenging activity (A-RA), ferric reducing antioxidant power (FRAP), and metal chelating activity (MC-A) as described by Buamard et al. (2024).

For D-RA, DPPH solution in 60% ethanol was used as a source of radicals. The absorbance of reaction solution was measured at 517 nm. A standard curve was obtained using trolox (10 to 60 μM). To perform the A-RA assay, working ABTS working solution was prepared. Standard curve of Trolox (10–600 μM) was used for calculation. The absorbance of reaction mixture was measured at 734 nm.

FRAP solution was prepared shortly before the use. The absorbance of reaction mixture was determined at 593 nm. Standard curve of Trolox (50–600 μM) was prepared. The activity was then computed. MC-A was examined using ferrozine. Absorbance of reaction mixture was read at 562 nm. The EDTA (10–60 μM) was used for preparation of standard curve.

D-RA, A-RA and FRAP were reported as μmol Trolox equivalent /g of dry extract (μmol TE/g dry extract), while MC-A was expressed as μmol of EDTA equivalents per g of dry extract (μmol EE/g dry extract).

2.3.4. LC/MS profiling and identification

Qualitative analysis of compounds in the KLE-D was done using liquid chromatography-quadrupole time-of-flight mass spectrometry (LC-QTOF MS; 1290 Infinity II LC-6545 Q-TOF, Agilent Technologies, Santa Clara, CA, USA) following the method of Tagrida and Benjakul (2020). The compounds were considered putatively identified, based on the available LC-QTOF-MS/MS database.

2.3.5. Determination of color

Color analysis of both KLE and KLE-D was performed using a colorimeter (HunterLab Colorflex, Hunter Associates Laboratory, Reston, VA, USA) (Olatunde et al., 2018). L^*, a^* and b^* values were measured.

2.4. Effect of KLE-D at different levels on property and oxidative stability of sardine surimi gel during the refrigerated storage

2.4.1. Preparation of surimi gel

Surimi was defrosted overnight in a cold room (0–2 °C) before being chopped into small pieces. Thereafter, the chopped surimi was mixed with 2.5% (w/w) salt for 2 min using a mixer (National Model MK-5080 M, Selangor, Malaysia). KLE-D was then added into the paste to obtain varying levels (0.025–0.125%, w/w), calculated based on the total weight of the surimi paste having final moisture content of 80%. Thereafter, distilled water was used to adjust the moisture content to 80% and the mixture was then chopped for another 3 min. The obtained paste was stuffed into polyvinylidene chloride casings (2.5 cm in diameter) and the casings were tied. All preparations were carried out below 10 °C. Gels were prepared by setting (at 40 °C for 30 min), followed by heating (at 90 °Cfor 20 min), and cooling in iced water for

30 min. The gels were stored at 4 °Cfor 20 h before analyses.

2.5. Characterization of surimi gels added with and without KLE-D at varying levels

2.5.1. Breaking force (BF) and deformation (DF)

BF and DF of the surimi gel (diameter: 2.5 cm; thickness: 2.5 cm) were measured using a texture analyzer (Model TA-XT2, Stable Micro-Systems, Surrey, UK) as tailored by Buamard et al. (2024). The gel was tested using a spherical plunger. BF and DF, representing mechanical strength and flexibility, were recorded.

2.5.2. Expressible moisture content (EMC)

EMC of surimi gel was measured and computed using the following formulation (Murugesan et al., 2025):

$$\textit{Expressible moisture content}\ (\%) = \frac{(A-B)}{A} \times 100\%$$

where A and B represent the weights of surimi gel before and after pressing with the standard weight (5 kg) for 2 min.

2.5.3. Determination of whiteness

Measurements of L^*, a^* and b^* values were performed. Subsequently, the whiteness was calculated (Park, 2005):

$$\text{Whiteness} = 100 - \left[(100 - L^*)^2 + a^{*2} + b^{*2}\right]^{0.5}$$

2.5.4. Textural profile analysis (TPA)

Chewiness, hardness, gumminess, springiness, and cohesiveness of the gels were assessed with a TA-XT2 texture analyzer equipped with a 50 kg load cell and a cylindrical aluminum probe measuring 50 mm in diameter. During TPA, the crosshead moved at 0.5 mm/s, compressing each sample twice to half its initial height with a 10 s pause between compressions.

2.5.5. Fourier transform infrared attenuated total reflection spectroscopy (FTIR-ATR)

The samples were analyzed by ATR-FTIR (ALPHA-FTIR, Bruker, Bremen, Germany) to examine their functional groups and chemical bonds. Spectra spanning 4000–500 cm^{-1} were acquired at 4 cm^{-1} resolution using 32 scans at ambient temperature. The spectra were baseline-normalized in OPUS 7.0.7 (Bruker). Changes in protein secondary structure were assessed by deconvoluting the amide I region (1600–1700 cm^{-1}) with PeakFit 4.12. After linear baseline subtraction, component bands within the amide I region were identified in the second-derivative spectrum (using Savitzky–Golay smoothing with a software-selected level) and fitted with a Gaussian peak-shape function using automatically estimated initial amplitudes. Peak position, width, and amplitude were determined, with all fits achieving R^2 of approximately 0.99. The bands at 1618–1640, 1640–1650, 1650–1660 and 1660–1690 cm^{-1} were assigned to β-sheet, random coil, α-helix and β-turn structures, respectively. The relative content of each secondary structure was calculated as the percentage of its fitted peak area relative to the total amide I band area.

2.5.6. Dynamic rheology

Surimi pastes from CON, KLE-D0.1, and KLE-D0.125 formulations were used for dynamic rheological measurements. Storage modulus (G′) was recorded with a HAAKE RheoStress1 rheometer (Thermo Fisher Scientific, Karlsruhe, Germany) using a 35 mm probe and a 2° cone-and-plate geometry. The paste was loaded onto the plate with the measurement gap set to 1 mm. The excess paste at the edge of the geometry was trimmed prior to measurement. Strain and oscillation frequency were set at 1% and 1 Hz, respectively. A preliminary oscillatory amplitude sweep confirmed that parameters fell within the linear viscoelastic region. The temperature sweep was then immediately initiated without an equilibration hold period. During the temperature sweep, samples were heated from 20 to 90 °C at 1 °C/min. Their surfaces were covered with silicone oil to limit evaporation during measurement.

2.5.7. Microstructure

Surimi gel specimen (2–3 mm thick) were fixed in phosphate buffer (100 mM, pH 7.4) containing 2.5% glutaraldehyde. Dehydration was carried out through an ethanol series (Buamard et al., 2024). The specimens were gold-coated and examined at 10,000× magnification with Quanta 400 SEM (FEI, Eindhoven, The Netherlands).

2.6. Effect of KLE-D on lipid oxidation of surimi gel during refrigerated storage

The surimi gels with and without KLE-D at 0.1% (w/w) were prepared. The gel samples were then packed in a polypropylene zip-lock bags. The gel samples were stored at 4 °C and analysed on days 0, 4 and 8. Peroxide value (PV) and thiobarbituric acid-reactive substances (TBARS) were evaluated (Sae-Leaw et al., 2016).

2.7. Statistical analysis

Completely randomized design (CRD) was opted for the whole experiment. The resulting data were analyzed using one-way and two-way ANOVA. The significant differences among means were examined using Duncan's multiple range test. For pair comparison, a t-test was employed. Statistical analyses were performed with SPSS for Windows (SPSS Inc., Chicago, IL, USA), and differences were considered statistically significant at $p < 0.05$.

3. Results and discussion

3.1. Chlorophyll, color, phenolic content, and antioxidant activity of Kenikir leaf extract with and without dechlorophyllization

3.1.1. Extraction yield and recovery following dechlorophyllization

KLE had an extraction yield of 6.40% (based on dry leaf powder). Following dechlorophyllization, the extract solid mass was 71.88% of the original extract mass, equivalent to an extraction yield of 4.60% (based on dry leaf powder). The lower mass of KLE-D indicated that some compounds might have been co-precipitated with chlorophyll. As a consequence, the less compounds were retained in the top layer. Extraction yields of *C. caudatus* varied with the extraction procedure and operating conditions (Latiff et al., 2021; Moshawih et al., 2017). Therefore, the yield of KLE was affected by dechlorophyllization, during which some hydrophobic compounds could be lost in the sediment during the precipitation process.

3.1.2. Chlorophyll content and color

Dechlorophyllization affected the chlorophyll content and color of kenikir leaf extract (KLE). This process decreased the chlorophyll a, chlorophyll b, and total chlorophyll contents in KLE (Table 1). The chlorophyll content in KLE-D was 0.043 mg/g, while KLE had a content of 0.254 mg/g. Chlorophyll b content in KLE decreased from 0.095 mg/g to 0.073 mg/g after dechlorophyllization. These decreases directly led to a reduction in total chlorophyll content from 0.330 mg/g in KLE to 0.112 mg/g in KLE-D. These results showed that the dechlorophyllization process was effective in removing chlorophyll, a green pigment, especially chlorophyll a, which is the dominant pigment and gives the extract a dark green color (Dębczak et al., 2024). Chlorophyll a was removed to a greater extent during the dechlorophyllization process than chlorophyll b, resulting in a greater decrease compared with chlorophyll b (Singh et al., 2023). The reduction in chlorophyll content directly affected the color characteristics of the extract. The significantly higher brightness value (L^*) was found in KLE-D (8.19) than in KLE

Table 1
Chlorophyll content, color parameters, total phenolic content and antioxidant activities of ethanolic kenikir leaf extract (KLE) with and without dechlorophyllization (KLE-D) by sedimentation method.

Parameters	KLE	KLE-D
Chlorophyll a (mg/g)	0.254 ± 0.014a	0.043 ± 0.004b
Chlorophyll b (mg/g)	0.095 ± 0.002a	0.073 ± 0.003b
Total Chlorophyll (mg/g)	0.330 ± 0.015a	0.112 ± 0.008b
L^*	7.813 ± 0.085b	8.196 ± 0.129a
a^*	−0.33 ± 0.03a	0.37 ± 0.02b
b^*	−3.11 ± 0.29a	−1.83 ± 0.06b
Total phenolic content (mg GAE/g)	288.39 ± 27.45a	298.40 ± 25.19a
D-RA (μmol TE/g)	56.63 ± 0.37b	59.23 ± 0.13a
A-RA (μmol TE/g)	60.30 ± 2.18a	58.99 ± 1.45a
FRAP (μmol TE/g)	51.95 ± 1.27a	52.39 ± 0.80a
MC-A (μmol EE/g)	9.84 ± 0.23a	9.91 ± 0.47a

Values are mean ± standard deviation (n = 3). Different lowercase letters within the same row indicate a significant difference ($p < 0.05$). A-RA: ABTS radical scavenging activity, D-RA: DPPH radical scavenging activity, FRAP: Ferric reducing antioxidant power, MC-A: Metal chelating activity.

(7.81), indicating that the extract became lighter after dechlorophyllization (Tagrida & Benjakul, 2021). This increase in the L^* value was in line with the reduction of chlorophyll pigment. The value of a^* changed from negative in KLE (−0.33) to positive in KLE-D (0.37), indicating a shift in color from a green tendency toward a slightly reddish hue. This confirmed that chlorophylls, as the primary green pigment, were substantially removed due to dechlorophyllization (Singh et al., 2023). Nonetheless, the b^* value increased from −3.11 to −1.83, indicating a decreased intensity of the bluish color associated with a more neutral color. These changes in the values of a^* and b^* suggested that dechlorophyllization not only lowered the intensity of the greenish color but also yielded the extract with lighter color. This made the resulting extract (KLE-D) become more visually acceptable. Overall, these results showed a strong relationship between chlorophyll content and color parameters (Tsuchiya et al., 2025). The lower the chlorophyll content, specifically chlorophyll a and total chlorophyll contents, the lighter color and the less green color were achieved. Dechlorophyllization has been shown to be a powerful tool in improving the color of plant extracts by reducing chlorophyll pigments without negligibly eliminating other bioactive components (Singh et al., 2023; Sinlapapanya et al., 2023). Thus, the dechlorophyllization had the potential to improve the visual appearance of the KLE, making it more suitable for food applications without causing the undesirable discoloration in the resulting food products.

3.1.3. Total phenolic content and antioxidant activities

Dechlorophyllization had no influence on total phenolic content (TPC). Most antioxidant activities tested by all assays of the KLE-D extract were not markedly affected by the dechlorophyllization process (Table 1). No differences in TPC values between KLE (288.39 ± 27.45 mg GAE/g) and KLE-D (298.40 ± 25.19 mg GAE/g) were observed ($p > 0.05$). Although the TPC concentration of KLE-D was numerically higher than that of KLE, the difference was not statistically significant ($p > 0.05$). KLE-D had a total phenolic recovery of 74.37% relative to KLE. This result indicated that some phenolic compounds, especially those with hydrophobic characteristics, were co-precipitated with chlorophyll as shown by the lower recovery. Moreover, the Folin–Ciocalteu assay estimates reducing capacity rather than selectively quantifying all phenolic molecules. Consequently, the calculated recovery should be interpreted as Folin–Ciocalteu-based phenolic recovery (Raposo et al., 2024). Based on the Folin–Ciocalteu assay, TPC might be over-estimated since any reducing agents were able to reduce the reagent, causing the high calculated TPC value. This is considered a limitation of the assay used. When the chlorophylls were removed, some non-polar phenolic compounds might also have been eliminated via co-precipitation with water. As a consequence, dechlorophyllization could lower total chlorophyll and increased lightness (L^*) without causing a significant loss of TPC. Proper dechlorophyllization was able to reduce green pigment without lowering the main phenolic fraction, as most phenolics were still retained in the upper phase (water phase) during chlorophyll removal (Olatunde et al., 2018).

Higher D-RA activity was found in KLE-D (59.23 ± 0.13) than that of KLE (56.63 ± 0.37) ($p < 0.05$), indicating that dechlorophyllization increased the hydrogen-donating capacity to DPPH radicals. Chlorophyll under certain conditions has been reported to act as a prooxidant or to decrease the stability of phenolic antioxidant compounds (de Carvalho & Nunes, 2021; Ebrahimi et al., 2024). In addition, the reduction in chlorophyll content might augment the proportion of active antioxidative compounds in the extract, thereby increasing its antioxidant capacity of the extract (Namal Senanayake, 2013). In addition, the presence of chlorophyll in plant extracts likely limits their application in food and biological systems due to its effects on color and potential prooxidative activity. Therefore, effective dechlorophyllization is strongly recommended for decreasing the green color caused by chlorophyll (Singh et al., 2023). In contrast, A-RA and FRAP showed no noticeable differences between KLE and KLE-D ($p > 0.05$). It was suggested that the antioxidant capacity of the ABTS system, which has been used to examine amphiphilic antioxidants, and the reduction ability of Fe^{3+} ions in the FRAP test, were relatively stable after dechlorophyllization was adopted. In general, A-RA and FRAP were highly correlated with TPC. However, the antioxidant activity of plant extracts can be decreased only when dechlorophyllization process also removed the phenolic compounds with antioxidant activity (Paixao et al., 2007). In addition, no differences in MC-A between KLE and KLE-D were observed. Thus, phenolic functional groups that bind transition metal ions, such as Fe^{2+}, were not significantly affected by the dechlorophyllization process. MC-A represents the ability in chelation or deactivation of transition metals, serving as prooxidant. Collectively, the dechlorophyllization method used in the present study did not show negative impact on antioxidant activity of KLE-D.

3.1.4. Identification and profiling of active compounds in KLE-D

The phytochemical composition of KLE-D was determined using LC-QTOF-MS/MS in both negative and positive electrospray ionization (ESI) modes. The identified compounds with their molecular formula, m/z values, molecular masses and relative abundances are summarized in Table 2. More compounds were detected in the negative ion mode than in the positive ion mode, suggesting that KLE-D consisted mostly of acidic polyphenolic compounds that readily formed deprotonated ions. This result was consistent with earlier research, in which phenolic acids and flavonoids tended to have better ionization efficiency and sensitivity in the negative ESI mode due to their hydroxyl and carboxyl functional groups (J. Liu et al., 2021; Rompas et al., 2025).

Nineteen compounds were found in the negative ion mode, while five compounds were detected in the positive ion mode. The most abundant metabolites were 1,2,3-trihydroxybenzene, galactonic acid, 6-O-methylarmillaridin, irisxanthone and 5,7,3′,4′,5′-pentahydroxy-3,6,8-trimethoxyflavone. 1,2,3-trihydroxybenzene or pyrogallol, comprises a six-carbon benzene ring with three hydroxyl (-OH) groups attached to three adjacent carbon atoms (Gier et al., 2022). All of the aforementioned compounds contain multiple hydroxyl groups. Other notable phytochemicals were tricetin 3′-xyloside, mangiferin 6′-gallate, theogallin, 4-glucogallic acid, quercetin, sinapoyltartronate and apigenin 7-rhamnosyl-(1→2)-galacturonide. In the positive ion mode, the major component was cyanidin. Quercetin was reported to increase the gel strength of CHOS-enriched pangasius surimi (Pati et al., 2026). Some compounds contained ketone functional groups, e.g. Irisxanthone (Bukvički et al., 2018) or 5,7,3′,4′,5′-pentahydroxy-3,6,8-trimethoxyflavone (Elhewehy et al., 2025). Some identified compounds contained carbonyl groups that might contribute to interactions with proteins and serve as hydrogen-bond acceptors. Some compounds possessing OH groups could act as hydrogen donor. The benzene ring was able to

Table 2
Active compounds present in the dechlorophyllized ethanolic extract of kenikir leaf (KLE-D).

Compounds	Formula	*m/z*	Mass (g/mol)	Abundance ($\times 10^6$)
Negative ion mode analysis				
1,2,3-Trihydroxybenzene	$C_6H_6O_3$	125.02	126.03	3.42
Galactonic acid	$C_6H_{12}O_7$	195.05	196.06	3.31
6-O-Methylarmillaridin	$C_{25}H_{31}ClO_6$	445.18	462.96	3.04
Irisxanthone	$C_{20}H_{20}O_{11}$	435.09	436.10	2.88
5,7,3′,4′,5′-Pentahydroxy-3,6,8-trimethoxyflavone	$C_{18}H_{16}O_{10}$	392.07	392.32	2.63
Tricetin 3′-xyloside	$C_{20}H_{18}O_{11}$	433.08	434.09	1.71
Hydroquinone	$C_6H_6O_2$	109.03	110.04	1.49
Mangiferin 6′-gallate	$C_{26}H_{22}O_{15}$	573.09	574.10	1.27
Lippioside II	$C_{25}H_{30}O_{14}$	553.16	554.16	1.24
Mascaroside	$C_{26}H_{36}O_{11}$	523.22	524.23	1.14
Desmethyldehydroamlodipine	$C_{19}H_{21}ClN_2O_5$	391.11	392.11	1.12
Theogallin	$C_{14}H_{16}O_{10}$	343.07	344.07	1.10
Citric acid	$C_6H_8O_7$	191.02	192.03	0.87
4-Glucogallic acid	$C_{13}H_{16}O_{10}$	331.07	332.07	0.81
Rumexoside	$C_{20}H_{22}O_{10}$	421.11	422.12	0.78
Quercetin	$C_{15}H_{10}O_7$	301.04	302.04	0.73
Sinapoyltartronate	$C_{14}H_{14}O_9$	325.06	326.06	0.71
Apigenin 7-rhamnosyl-(1->2)-galacturonide	$C_{27}H_{28}O_{15}$	591.14	592.14	0.69
Oleoside 11-methyl ester	$C_{17}H_{24}O_{11}$	403.12	404.13	0.68
Positive ion mode analysis				
Cyanidin	$C_{15}H_{11}O_6$	287.06	287.06	0.52
Maclurin 3-C-(6″-p-hydroxybenzoyl-glucoside)	$C_{26}H_{24}O_{13}$	545.13	544.12	0.42
5,2′,4′-Trihydroxy-3,6,7,8-tetramethoxyflavone	$C_{19}H_{18}O_9$	391.10	390.10	0.32
5-Hepten-3-yn-1-ol, 2,2-dimethyl-7-[methyl(1-aphthalenylmethyl)amino]-, (E)-	$C_{21}H_{25}NO$	325.23	307.19	0.29
Cytosine	$C_4H_5N_3O$	112.05	111.04	0.24

interact with protein side group via hydrophobic interaction. Other leaves have been documented to be the potential sources of active compounds. Quercetin 3-(2-galloylglucoside), methyl 2,4,6-trihydroxybenzoate and isorhamnetin 4′-O-glucuronide were reported to be abundant compounds in ethanolic Jik leaf extract (Ahmad et al., 2024). Dechlorophyllized ethanolic extract of Betel and Chaphlu leaves had vitexin 4′-O-galactoside and isovitexin as the most abundant compounds, respectively (Tagrida & Benjakul, 2020). Overall, KLE-D was rich in phenolic acids, flavonoids, flavonoid glycosides, xanthones and other polyhydroxylated metabolites.

The high abundance of these polyphenolic compounds is particularly significant because their numerous hydroxyl groups which can provide the proton or electron to radicals, thus lowering oxidative reaction. A number of plant metabolites, including quercetin Shen et al. (2025), cyanidin Liu et al. (2024), mangiferin derivatives (Kaur et al., 2020) and gallic acid derivatives (Doğan Ulu et al., 2026) are well-known antioxidants. These compounds have strong antioxidant effects through the scavenging reactive oxygen species and chelation of transition metals, thereby reducing the lipid oxidation in several systems (Wu et al., 2022).

Furthermore, these compounds, particularly those containing hydroxyl groups or benzene rings were able to interact with myofibrillar proteins through hydrogen bonding and hydrophobic interactions, respectively, thereby promoting protein aggregation and strengthening the gel network. Flavonoids, including quercetin, derivatives of tricetin and mangiferin were also shown to alter the protein conformation and promote intermolecular interactions between protein chains (Tagrida & Benjakul, 2020).

3.2. Effect of KLE-D at different levels on the textural properties of sardine surimi gel

3.2.1. Breaking force (BF) and deformation (DF)

BF and DF of surimi gel increased with the addition of KLE-D up to a concentration of 0.1% ($P < 0.05$) and subsequently decreased at a higher concentration (0.125%) (Fig. 1A, B). The addition of 0.1% KLE-D resulted in the highest BF (~100 g), in which an increase of about 25% was achieved, compared to that of control. The highest DF (~1.9 mm), was also obtained with addition of 0.1% KLE-D, representing an increase of about 46%, compared to the control. However, KLE-D at high concentration (0.125%) resulted in the decreases in both BF and DF. Increases in BF and DF of sample added with 0.1% KLE-D indicated the enhanced gel strength and deformation capacity, potentially linked to alterations in protein network organization. Previous research has proposed that phenolic compounds may interact with myofibrillar proteins via non-covalent interactions, such as hydrogen bonding and hydrophobic interactions (Buamard et al., 2024). However, these interactions were not directly assessed in the current study. At a higher concentration of 0.125% KLE-D, the observed decreases in BF and DF implied that excessive extract addition had a negative impact on gel formation. Phenolic self-association and alterations in protein aggregation were possible explanations (Buamard et al., 2024), though these mechanisms warrant further investigation.

3.2.2. Expressible moisture content (EMC)

EMC decreased with increasing KLE-D concentration up to 0.1% (Fig. 1C). Nonetheless, the addition of 0.125% KLE-D led to an increase in EMC ($p < 0.05$). No difference in EMC was found between the samples containing 0.025–0.075% and 0.125% KLE-D ($p > 0.05$). A reduction of EMC to the lowest value (~18.5%) at 0.1% KLE-D indicated a significant increase in the water holding capacity (WHC) of gel matrix, which was in line with the increases in BF and DF at the same concentration used. The lowered EMC suggested that surimi gel strengthened by phenolic compounds had a denser and more organized gel matrix, allowing water to be entrapped more effectively. Surimi gels with strong and homogeneous protein networks generally exhibited higher water-holding capacity (Duan et al., 2023; Z. Wu et al., 2025). However, an increase in EMC in the gel containing 0.125% KLE-D indicated a decrease in the ability of gel network to retain water. This was thought to be due to the excessive phenolic–protein interactions and phenolic self-aggregation, resulting in a less homogeneous, and looser gel structure. As a consequence, water could be expressed and released from the gel network under pressure with ease, as evidenced by the increased EMC (Wu et al., 2025)

3.2.3. Whiteness

The whiteness value of surimi gel showed a relatively stable trend when KLE-D at low to medium concentrations (0–0.075%) was applied. However, a decrease in whiteness was found when KLE-D at 0.1% and 0.125% was incorporated ($p < 0.05$) (Fig. 1D). Overall, gels added with KLE-D at low concentrations showed negligible changes in whiteness. Conversely, a decrease in the whiteness of gel added with KLE-D at the concentration of ≥0.1% indicated that phenolic compounds, especially flavonoids, which have naturally yellowish to brownish color, could reduce the whiteness of surimi gel (Borderías et al., 2020). This

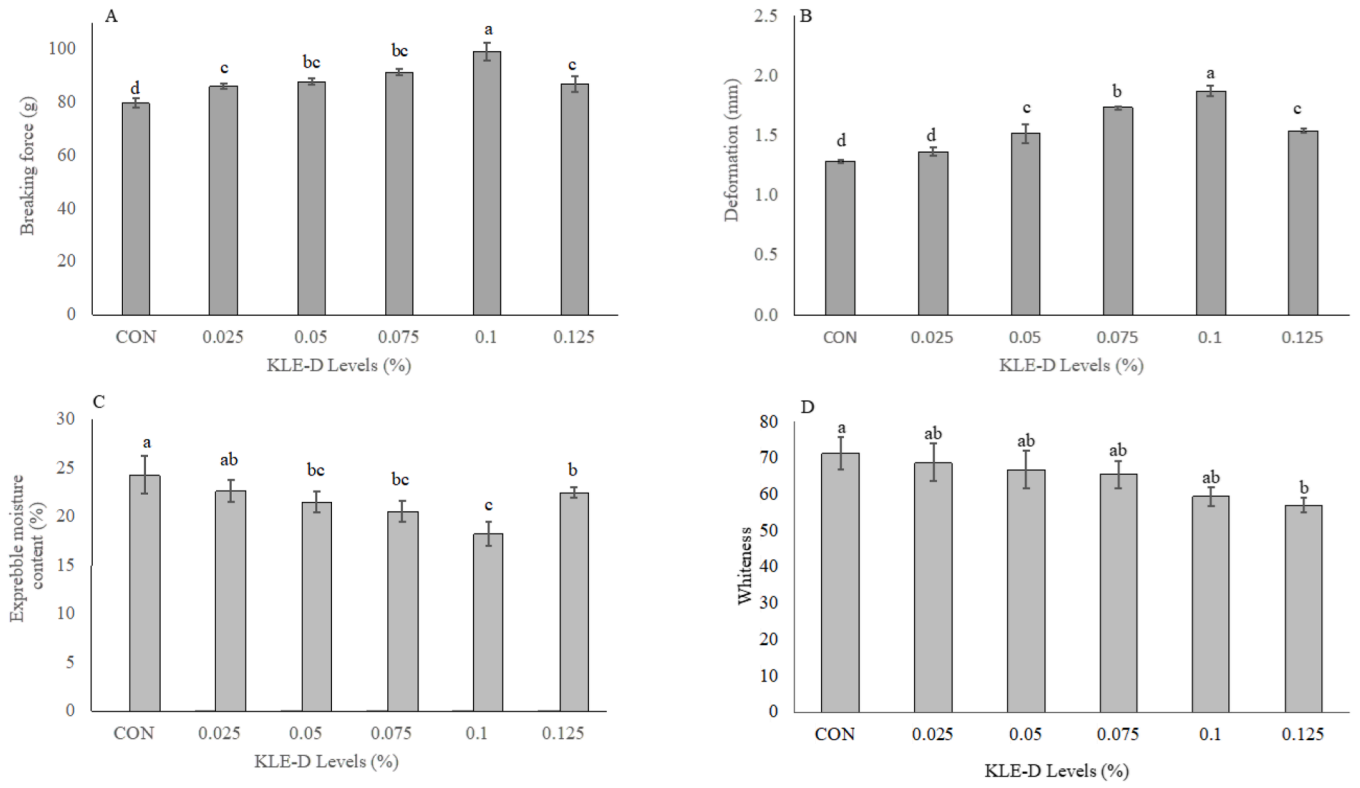

Fig. 1. Breaking force (A), deformation (B), expressible moisture content (C) and whiteness (D) of sardine surimi gel added with and without KLE-D at different levels. Vertical bars represent the standard deviation (n = 3). Different lowercase letters on the bar indicate significant differences ($p < 0.05$). KLE-D: Dechlorophyllized kenikir leaf extract.

phenomenon has been consistently reported when phenolic-rich plant extracts were added to surimi gels, resulting in decreased gels whiteness, especially with increasing phenolic concentrations (Wu et al., 2022). Moreover, the residual phenolic compounds might undergo oxidation, leading to the formation of brownish quinone (M.-H. Park et al., 2026). This might lead to the lowered whiteness of surimi gel. Therefore, KLE-D at 0.075–0.1% significantly improved the mechanical and WHC properties of the gel, although the 0.1% treatment significantly reduced whiteness of resulting gel.

3.3. Effect of KLE-D at the selected concentrations on textural properties, FTIR spectra, rheology and microstructure of surimi gels

3.3.1. Textural properties

Textural properties of surimi gel added with and without KLE-D at the optimal level (0.1%) and an excessive level (0.125%) were different (Table 3). The addition of 0.1% KLE-D to sardine surimi gel resulted in increases in hardness, springiness, gumminess, and chewiness ($p < 0.05$). However, all the aforementioned parameters decreased when KLE-D at 0.125% was incorporated ($p < 0.05$). Nonetheless, similar cohesiveness values were found among all the samples, irrespective of KLE-D levels ($p > 0.05$). Increased hardness suggested that the phenolic compounds in KLE-D, at an optimal concentration, were able to strengthen gel network, whereas at higher concentration, the detrimental effect was attained. A similar phenomenon has been reported in polyphenol-enriched myofibrillar protein gel systems, where the increased hardness was found at moderate concentrations of polyphenols due to optimal phenolic–protein interactions (Buamard & Benjakul, 2015). At high concentrations, the irregular protein aggregation occurred, leading to lower gel strength (Cheng et al., 2021).

Springiness of surimi gel also increased when 0.1% KLE-D was added, indicating the upsurged gel elasticity. The increase in springiness indicated the improved recovery of the gel after deformation (Zhang et al., 2019) This result suggested that KLE-D incorporation affected the mechanical behavior of the gel network. Nonetheless, the present measurements did not establish whether this improvement resulted directly from phenolic–protein interactions. However, the decrease in springiness of gel was found in the presence of KLE-D at 0.125%. Excessive aggregation of proteins led to the formation of coagulum type gel with poorer mechanical property.

The cohesiveness values were similar among different samples ($p > 0.05$), indicating that the internal integrity or cohesion of protein chains in gel matrix was relatively stable. Shi et al. (2021) reported that polyphenol addition had a greater effect on the mechanical properties of macro gels than on the internal cohesion of protein network.

Gumminess and chewiness showed the same trend with hardness, which increased significantly when 0.1% KLE-D was incorporated and decreased when an excessive concentration of KLE-D (0.125%) was

Table 3
Textural profile of sardine surimi gel with and without KLE-D at the selected levels.

KLE-D concentrations (%, w/w)	Hardness (g)	Springiness (cm)	Cohesiveness	Gumminess (g)	Chewiness (g.cm)
0	686.87 ± 33.62b	0.69 ± 0.04b	0.23 ± 0.01a	165.58 ± 12.21b	106.55 ± 4.40b
0.1	779.67 ± 36.19a	0.80 ± 0.01a	0.24 ± 0.01a	201.28 ± 13.61a	132.65 ± 4.93a
0.125	711.12 ± 26.26ab	0.77 ± 0.03ab	0.22 ± 0.02a	170.18 ± 5.44b	119.57 ± 5.36ab

Values are mean ± standard deviation (n = 3). Different lowercase letters within the same column indicate a significant difference ($p < 0.05$).

used. Since gumminess and chewiness are derived from hardness and springiness, the increases in these parameters reflect the greater energy required for gel deformation and chewing (Fatan Tikmedash et al., 2026; Ma et al., 2024). The elevated levels of gumminess and chewiness in 0.1% KLE-D added sample were consistent with the enhancement of the gel textural properties. In contrast, the decreases in both parameters for gel containing 0.125% KLE-D indicated that the extract at an excessive concentration might not be favorable for gel formation. Such an observation could be explained by phenolic self-association; however, this mechanism was not directly investigated in the present work. Further investigation is still required.

3.3.2. FTIR spectra and secondary structure

The FTIR spectra of KLE-D and sardine surimi gels containing different concentration of KLE-D are shown in Fig. 2A. KLE-D displayed a broad absorption band at 3313 cm^{-1} which generally associated with O–H stretching of phenolic hydroxyl groups (Aminu et al., 2021). The band at 2932 cm^{-1} was attributed to aliphatic C–H stretching, whereas band at 1687 and 1563 cm^{-1} were associated with conjugated C═O stretching and aromatic skeletal vibrations, respectively. The prominent bands at 1042 and 1015 cm^{-1} represented C–O and C–C stretching vibrations in the fingerprint region. All surimi gels showed the typical protein bands at Amide A, Amide B, Amide I and Amide II region. CON showed the amide A-associated band at 3294 cm^{-1}, whereas the bands of KLE-D0.1 and KLE-D0.125 samples were observed at 3297 cm^{-1} and 3313 cm^{-1}, respectively. The Amide A band is associated with N–H stretching vibrations that can be influenced by hydrogen bonding (Pielesz et al., 2011). The difference between the control (3294 cm^{-1}) and the sample containing 0.1% KLE-D (3297 cm^{-1}) was only 3 cm^{-1}. Because this difference is smaller than the reported spectral resolution of 4 cm^{-1}, it cannot be interpreted confidently as a significant band shift (Panpipat et al., 2023). Therefore, this difference was not considered for altered hydrogen bonding or direct phenolic–protein interactions. The band observed at 3313 cm^{-1} in the sample containing 0.125% KLE-D might reflect a change in the vibrational environment; however, this observation alone did not establish a specific molecular interaction. Therefore, the FTIR results should be interpreted in light of the secondary structure, rheological, and microstructural results, but not in terms of a specific molecular mechanism. However, the O–H/N–H peak at a higher concentration (0.125% KLE-D) shifted to 3313 cm^{-1}, thus indicating greater interference with hydrogen bond. Excess phenolic molecules might undergo self-aggregation, thus remaining the less free hydroxyl groups for the formation of hydrogen bond. This was more likely associated with the less protein cross-linking in gel network. This structural interference generated a less compact and more fragmented network, leading to decreased textural integrity and reduced WHC.

The Amide B band remained at 2926–2927 cm^{-1} in all gel samples, indicating no marked change in the aliphatic C–H environment. Similarly, the Amide I and Amide II bands were consistently detected at 1656 and 1544 cm^{-1}, respectively. Amide I originates predominantly from C═O stretching of the peptide backbone and is particularly sensitive to protein secondary structure, whereas Amide II is mainly associated with

A

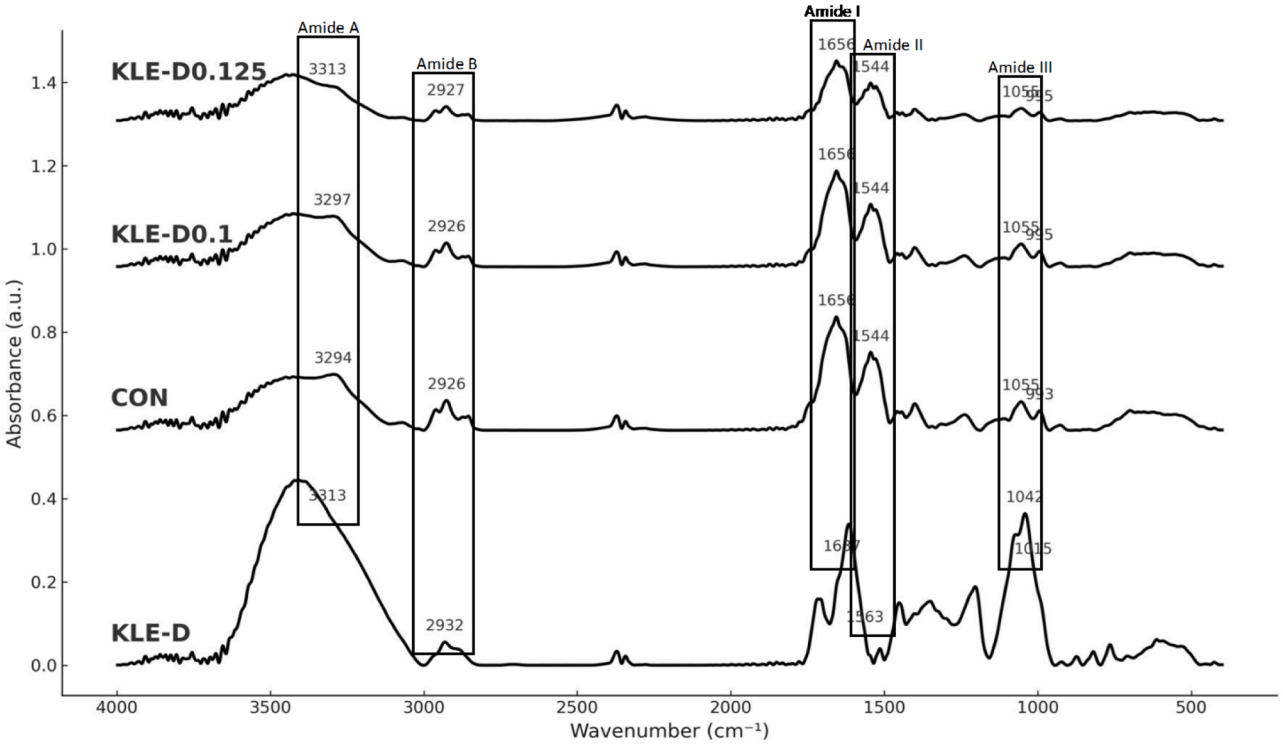

B

Secondary structure (%)	CON	KLE-D0.1	KLE-D0.125
β-sheet	33.79	32.81	33.64
Random coil	14.29	14.80	14.87
α-helix	30.85	31.34	31.76
β-turn	21.07	21.05	19.74

Fig. 2. FTIR spectra (A) and secondary-structure composition determined by deconvolution of the amide I region (B) of sardine surimi gels added with and without KLE-D at the selected levels. KLE-D: Dechlorophyllized kenikir leaf extract. KLE-D0.1 and KLE-D0.125: Surimi gel added with KLE-D at 0.1% and 0.125% (w/w), respectively. CON: surimi gel without the addition of KLE-D.

N–H bending coupled with C–N stretching (Awal et al., 2024). Although Amide I remained unchanged, deconvolution of the Amide I region revealed small differences in the relative secondary-structure composition (Fig. 2B). CON contained 33.79% β-sheet, 30.85% α-helix, 21.07% β-turn, and 14.29% random-coil structures. The results suggested that the β-sheet was the most abundant structure, followed closely by α-helix, indicating that both ordered structures contributed substantially to the heat-induced sardine surimi gel network. In surimi gelation, myosin α-helix can partially unfold during heating and transformed into β-sheet, β-turn, and random coil structures (Wei et al., 2018). At 0.1% KLE-D, the β-sheet content decreased slightly from 33.79% to 32.81%, whereas the α-helix and random-coil contents increased slightly to 31.34% and 14.80%, respectively. The β-turn content remained almost unchanged at 21.05%. Minor alterations in the relative proportions of secondary structures were noted along with enhancements in BF, DF, WHC, and the elastic modulus at a concentration of 0.1% KLE-D. These results implied that the inclusion of KLE-D was plausibly linked to modifications in protein conformation and the organization of the gel network. Nonetheless, the current data do not clarify whether these modifications stemmed from direct phenolic-mediated hydrogen bonding, hydrophobic interactions, covalent cross-linking, or indirect influences on protein aggregation. Generally, these interactions could plausibly increase the number or stability of junction zones without markedly changing the overall proportion of α-helix, β-sheet and β-turn structures. As a result, the high G′ value and the compact, homogeneous microstructure with small pores were observed in KLE-D0.1 (Fig. 3A, B). The β-sheet content was 33.64% in KLE-D0.125, while the α-helix and random coil content increased to 31.76% and 14.87%, respectively. On the other hand, the β-turn content of KLE-D0.125 decreased to 19.74%. The increase in random coil might reflect slightly greater conformational disorder, whereas the higher α-helix proportion could indicate the retention of some helical domains during heating. The results suggested that at the higher concentration, phenolic self-association or the excessive localized protein–phenolic interactions more likely promoted non-uniform aggregation, instead of well-organized protein-network formation. The results were in agreement with previous studies on phenolic-rich additives in surimi gels, where suitable levels enhanced protein cross-linking and gel network formation, while higher levels caused over-aggregation and poorer gel quality (Murugesan et al., 2025). At a low EGCG levels, the addition of EGCG in surimi gel favored secondary-structure transitions and improved gel properties, whereas higher EGCG concentrations caused excessive protein crosslinking and aggregation, resulting in poorer network formation, reduced gel strength, and lower water retention. The deconvolution results confirmed that addition of KLE-D modestly altered the secondary structure of sardine surimi proteins to some extent. Overall, the observed changes in secondary structure were associated with the improved gel properties, but they did not independently demonstrate phenolic-induced protein cross-linking.

3.3.3. *Dynamic rheology*

The control, 0.1%, and 0.125% KLE-D treatments were selected for dynamic rheological analysis in comparison with the untreated surimi paste. Those two treated samples represented the sample containing the effective concentration, which showed the highest gel strength and the sample added with an excessive KLE-D concentration, yielding the poorer gel, respectively.

Fig. 3A shows the change in the elastic modulus (G′) of sardine surimi paste with and without the addition of KLE-D at the selected concentrations during heating from 20 to 90 °C. All samples exhibited a typical thermal gelation profile of myofibrillar proteins, consisting of an initial aggregation phase (Han et al., 2014), a temporary destabilization phase, a main gelation phase (Du & Betti, 2016), and a decline phase at high temperatures (Liu et al., 2026). In the temperature range of 20–35 °C, the G′ value of all samples increased gradually. This increase indicated the formation of a weak initial protein network, primarily stabilized by hydrogen bonds and other non-covalent interactions between myofibrillar protein chains. At this stage, the proteins were still in a dispersed or partially unfolded state. As a consequence, the elastic structure formed was not permanent. Similar phenomena have been widely reported in the surimi and fish protein gel systems during the early stages of heating at low temperatures (Buamard & Benjakul, 2015). In the temperature range of about 40–43 °C, all samples showed a slight decrease in G′. This slight decline was widely associated with the activation of heat-activated proteases, such as cathepsins (Si et al., 2025). At

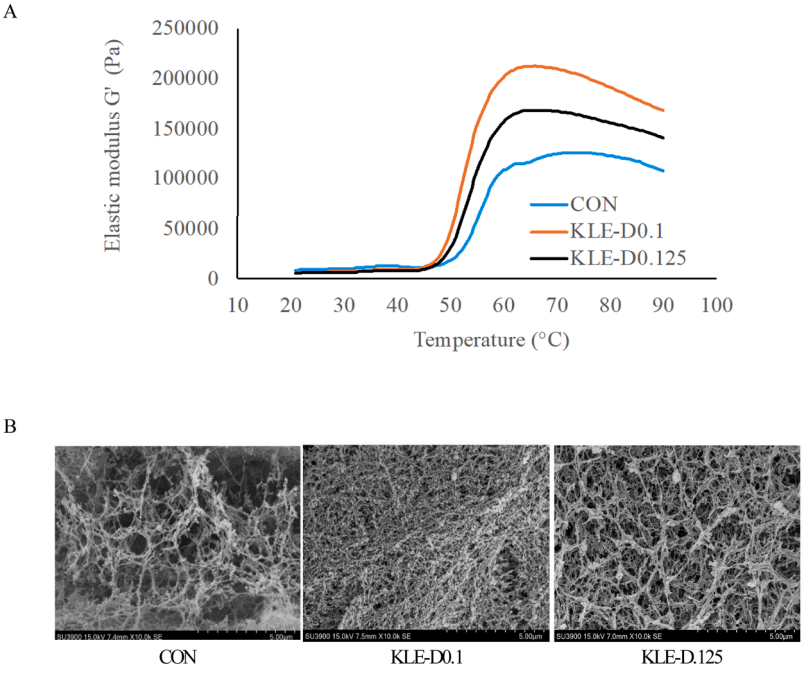

Fig. 3. Elastic modulus (G′) during heating (20–90 °C) (A) and scanning electron microscopic images (B) of sardine surimi gels added with and without KLE-D at the selected levels. KLE-D: Dechlorophyllized kenikir leaf extract. KLE-D0.1 and KLE-D0.125: Surimi gel added with KLE-D at 0.1% and 0.125% (w/w), respectively. CON: surimi gel without the addition of KLE-D.

this temperature, the protease became active and partially degraded myofibrillar proteins, especially in the myosin tail region, thereby reducing protein chain entanglement and continuity (Ding et al., 2024). However, in the presence of KLE-D, protein degradation might be impeded as confirmed FTIR spectra (Fig. 2A).

The activity of heat-activated protease caused partial disruption of the protein chain, which reduced the ability of the system to maintain an elastic response. This was reflected by a slight decrease in G′ before the formation of a stable gel network. In addition, the partial unfolding of proteins due to heating increased the mobility of protein chains and weakened the initial non-covalent bonds that had been formed, thereby amplifying the G′-decreasing effect of this pre-gelation phase (Gani et al., 2018). After passing through the destabilization phase, a sharp rise in G′ was observed at about 46–65 °C across all samples. This increase suggested the transition of the sol to a thermo-irreversible gel, which resulted from myosin denaturation and more regular aggregation of myofibrillar proteins. In this phase, denatured proteins interacted together to form a strong, elastic three-dimensional gel network (Mleko & Foegeding, 2000). In addition, in this temperature range, indigenous transglutaminase could induce the cross-linking of proteins via non-disulfide covalent bonds (Buamard et al., 2024), resulting in the higher G′ value.

Gels added with 0.1% KLE-D had the highest G′ value in this phase, indicating the formation of the most robust and organized gel network. These results were consistent with the highest values of BF, DF, hardness, gumminess, and chewiness when gel contained 0.1% KLE-D. Overall, the higher elastic modulus reflected the strengthening of the gel's internal structure, which contributed directly to the improvement of textural properties. At temperatures between 65 °C and 90 °C, the entire sample again showed a slight decrease in G′. This decrease was associated with contraction and reorganization of the gel network, as well as the potential for water release from the protein matrix at high temperatures. Although all samples experienced a decrease in G′, the final G′ value at KLE-D 0.1% remained higher than that of control and KLE-D 0.125%, indicating better elastic network stability. In contrast, 0.125% KLE-D showed a lower final G′ value, indicating that the addition of KLE-D at higher concentrations did not provide an additional strengthening effect. Decrease in G′ value with the excessive concentration of KLE-D (0.125%) was associated with the decreased BF and increased EMC (Fig. 1). The observed increase in G′ signified the alterations in the viscoelastic behavior of the surimi paste throughout the gelation process. While this finding aligned with the improvements in gel properties, rheological measurements alone were insufficient to verify the formation of specific phenolic–protein bonds or covalent cross-links.

3.3.4. Microstructure

The microstructure of sardine surimi gel with and without the addition of KLE-D at the selected levels (0.1% and 0.125%) is shown in Fig. 3B. Apparent differences in pore size, protein strand thickness, and strand connectivity were observed between the different gel samples, suggesting that KLE-D concentrations directly influenced the organization of myofibrillar protein networks during gelation. In the control sample (CON), the gel network appeared relatively irregular. Non-uniform voids and large protein strands with a relatively loose structure were observed. This morphology indicated that a three-dimensional network was formed, but the density and number of junction zones between proteins were still limited. More open structures generally had lower water-holding capacity and moderate gel strength, as large cavities facilitated water migration and release when the gel was pressurized. Porous microstructural patterns in the control surimi gel have also been reported in various surimi systems without the addition of gel network-strengthening compounds. These phenomena are often associated with lower BF and DF values as well as higher EMC (Buamard & Benjakul, 2015). In contrast, when 0.1% KLE-D was added, a much more compact and homogeneous network was developed as characterized by smaller pores, a more uniform distribution of cavities, finer and tightly interconnected protein strands. The network with higher density suggested that the addition of KLE-D at optimal concentrations could improve myofibrillar protein connectivity and aggregation, resulting in a more stable three-dimensional gel matrix. This denser and less porous structure was consistent with higher maximum G′ values during heating, as well as increased BF, DF, hardness, gumminess, and chewiness, along with decreased EMC. The compact and homogeneous microstructure observed at 0.1% KLE-D was consistent with the enhanced rheological and textural properties of the gel. These findings suggested that KLE-D influenced the organization of the gel network. However, SEM images did not directly reveal the formation of phenolic–protein bonds or protein cross-links. When the concentration of KLE-D was increased to 0.125%, the gel microstructure showed a coarser and less irregular network than that added with 0.1% KLE-D. For this sample, thicker protein strands, larger pores, and irregular distribution of cavities were found, indicating the formation of non-uniform protein aggregates. This coarser and heterogeneous structure suggested that the excessive amount of KLE-D could not increase myofibrillar protein linkage but instead interfered with the formation of an organized gel network. In general, the increased adequate spacing between protein strands and the excessive formation of aggregation zones, which reduce the efficiency of regular protein–protein interactions generally resulted in the poor gel network with larger cavities (Sharma et al., 2025).

The more open and non-uniform microstructure of KLE-D 0.125% was in agreement with the decrease in mechanical properties of the gel, including decreased BF and gumminess, as well as an increase in EMC. In addition, the lower elastic gel network in this sample was consistent with a lower final G′ value in dynamic rheology analysis. A similar phenomenon was documented in surimi gels enriched with plant extracts or bioactive compounds, where optimal concentrations yielded the finest microstructures, whereas the excessive concentrations of plant extract resulted in rough and irregular network with decreased textural property (Sharma et al., 2025).

3.4. Effect of KLE-D on oxidative stability of sardine surimi gels during refrigerated storage

Sample added with 0.1% KLE-D was selected for storage stability study in comparison with the control (without KLE-D). From Fig. 4A(PV) and Fig. 4B (TBARS), lipid oxidation of the control and gel added with 0.1% KLE-D, which yielded the gel with the best gelling property, increased significantly over 8 days of storage ($p < 0.05$). Treatment, storage time and interaction were found to be significant ($P < 0.05$). Lipid oxidation is commonly found in surimi products due to the high content of unsaturated fatty acids susceptible to oxidation during cold storage (Cai et al., 2017). Although washing was carried out to remove the sarcoplasmic proteins and some portion of fat from the fish mince, some fat and phospholipids can be retained. Those lipids could be oxidized rapidly due to the plenty of polyunsaturated fatty acids (PUFAs) (Ebrahimi et al., 2024). On day 0, the peroxide value (PV) of the two samples ranged from 22 to 23 meq hydroperoxide/kg gel (Fig. 4A). During storage, the PV of the control increased to 48–49 meq hydroperoxide/kg on day 8, which represented an increase of about 2.1–2.2 folds. In contrast, gels added with 0.1% KLE-D showed a PV of about 41–42 meq hydroperoxide/kg on day 8 with an increase of about 1.8 folds. Thus, the sample added with 0.1% KLE-D had the lower PV by 14–16% compared with the control at the end of storage.

On day 0, the TBARS values for both samples ranged from 3.5 to 3.7 mg MDA/kg of gel, with no noticeable difference (Fig. 4B), suggesting that the addition of KLE-D did not affect the initial oxidation. During storage, the TBARS value in the control increased to approximately 12.0 mg MDA/kg on day 8, corresponding to a 3.3-fold increase over the initial value (day 0). In contrast, in gels incorporated with 0.1% KLE-D, TBARS reached about 10.8–11.0 mg MDA/kg on day 8, which

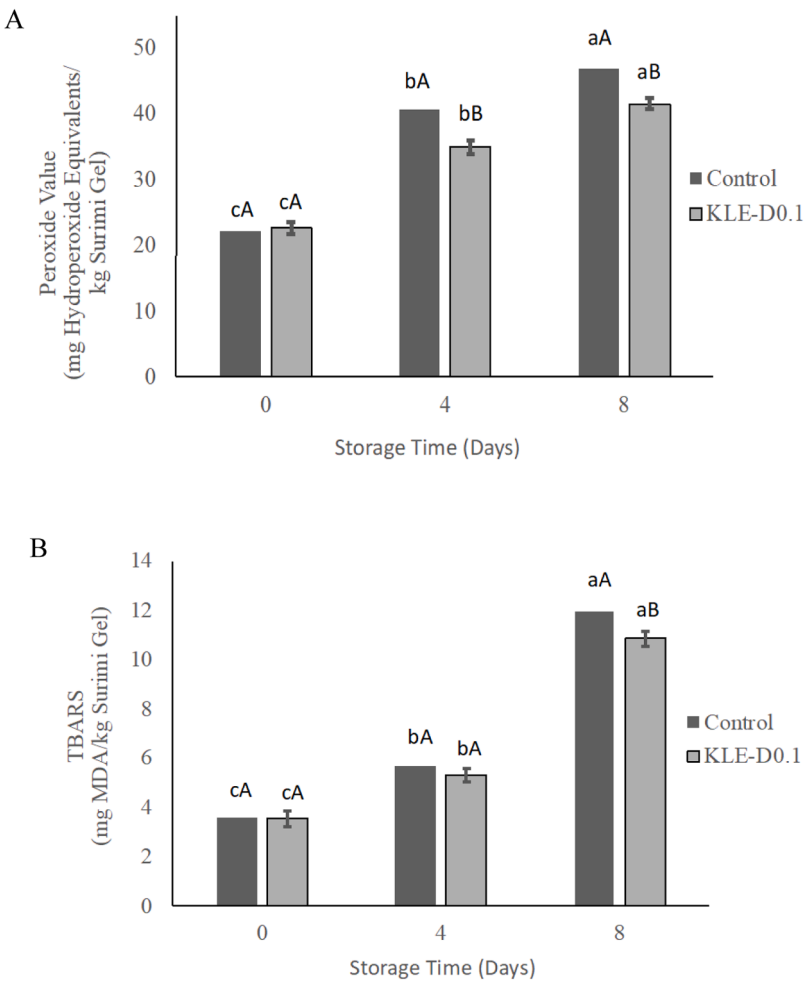

Fig. 4. Peroxide value (A) and TBARS value (B) of sardine surimi gel with and without 0.1% KLE-D (KLE-D0.1) during the refrigerated storage of 8 days. Vertical bars represent the standard deviation (n = 3). Different lowercase letters on the bars within the same sample indicate significant difference ($p < 0.05$). Different uppercase letters on the bars within the same storage time showed a significant different.

was 2.9-fold higher than the control. Thus, the addition of 0.1% KLE-D reduced TBARS formation of surimi gel during storage. The decrease in the formation of secondary oxidation products suggested that the phenolic compounds in KLE-D acted as effective chain-breaking antioxidants. Buamard et al. (2024) showed that the ethanolic extract of duea ching fruit, rich in phenolic compounds, significantly prevented the increase in TBARS values in sardine surimi during cold storage. This phenomenon aligned with several reports that plant phenolics could chelate prooxidant metals, stabilize peroxyl radicals and scavenge numerous radicals in fish protein-based products (Buamard et al., 2024). Quercetin contains multiple hydroxyl groups which can function as antioxidant (Qi et al., 2022).

4. Conclusion

Dechlorophyllization of ethanolic kenikir leaf extract using sedimentation effectively reduced chlorophyll content while maintaining a comparable total phenolic content and most antioxidant activities, while increasing DPPH radical-scavenging activity. Qualitative analysis of KLE-D by LC-QTOF-MS/MS indicated the presence of 24 tentatively identified compounds; 19 compounds were found in the negative ion mode, while 5 compounds were detected in the positive ion mode. The incorporation of KLE-D into sardine surimi gels significantly influenced gel properties in a concentration-dependent manner. Among the tested levels, 0.1% KLE-D was the optimal concentration, yielding the strongest gel network, highest elasticity, superior water-holding capacity, and the most compact microstructure. At this optimal level, the enhanced gel properties were associated with alterations in protein secondary structure, rheological behavior, and microstructural organization. Although KLE-D influenced gel network formation, the precise molecular interactions between polyphenols in the extract and myofibrillar proteins responsible for the gel strengthening remain unclear. Further studies using gel solubility analysis with different solubilizing solutions are needed to elucidate these interactions. In addition, the aggregation of myofibrillar proteins induced by the extract should be investigated *in vitro*. In contrast, higher KLE-D concentrations (0.125%) led to the reduced gel quality due to phenolic self-association or induction of coagulum gel. Furthermore, the addition of 0.1% KLE-D effectively retarded lipid oxidation of surimi gel during refrigerated storage, thereby improving the oxidative stability. Therefore, KLE-D could be used as the natural additive for improvement of quality and oxidative stability of sardine surimi gel. Before practical application, sensory evaluation, flavor and odor assessment, residual ethanol verification, microbiological safety, toxicological considerations, regulatory acceptability, and scale-up should be further studied.

CRediT authorship contribution statement

Muh Ali Arsyad: Writing – original draft, Methodology, Formal analysis, Data curation, Conceptualization. **Natchaphol Buamard:** Writing – review & editing, Methodology. **Mallikarjun Chanchi Prashanthkumar:** Writing – review & editing, Methodology, Data curation.

Umesh Patil: Writing – review & editing, Visualization, Software, Methodology. **Soottawat Benjakul:** Writing – review & editing, Visualization, Validation, Supervision, Resources, Project administration, Funding acquisition, Conceptualization.

Declaration of competing interest

The authors declare that they have not known competing financial interests or personal relationships that could have appeared to influence the work reported in this paper.

Acknowledgments

We appreciate the financial support provided by the Prince of Songkla University, Hat Yai, Thailand, under "PSU-Talent Management".

Data availability

Data will be made available on request.

References

Abidin, Z., Aminah, Razak, R., & Pratama, M. (2025). Phytochemical constituents, antioxidant and anti-inflammatory potentials of dechlorophyllized extract of kenikir leaves (*Cosmos caudatus* Kunth). *Tropical Journal of Natural Product Research*, 1958. https://doi.org/10.26538/tjnpr/v9i5.11

Ahmad, A. S., Sae-leaw, T., Zhang, B., & Benjakul, S. (2024b). Antioxidant and antimicrobial activities of Ethanolic Jik (*Barringtonia acutangula*) leaf extract and its application for shelf-life extension of Pacific white shrimp meat during refrigerated storage. *Food Control, 155*, Article 110037. https://doi.org/10.1016/j.foodcont.2023.110037

Aminu, N., Chan, S.-Y., Mumuni, M. A., Umar, N. M., Tanko, N., Zauro, S. A., Aminu, A., & Toh, S.-M. (2021). Physicochemical compatibility studies of triclosan and flurbiprofen with excipients of pharmaceutical formulation using binary, ternary, and multi-combination approach. *Future Journal of Pharmaceutical Sciences, 7*(1), Article 148. https://doi.org/10.1186/s43094-021-00302-7

Arsyad, M. A., Akazawa, T., & Ogawa, M. (2019). Effects of olive leaf powder on mechanical properties of heat-induced surimi gel. *Journal of Aquatic Food Product Technology, 28*, 2–13. https://doi.org/10.1080/10498850.2018.1559904

Awal, M. S., Benjakul, S., Prodpran, T., & Nilsuwan, K. (2024). Characteristics and properties of co-precipitated protein and film based on Bambara groundnut protein isolate and fish skin acid-soluble collagen. *Journal of Agriculture and Food Research, 18*, Article 101430. https://doi.org/10.1016/j.jafr.2024.101430

Ayuso, M., Carpena, M., Taofiq, O., Albuquerque, T. G., Simal-Gandara, J., Oliveira, M. B. P. P., Prieto, M. A., Ferreira, I. C. F. R., & Barros, L. (2022). Fig "*Ficus carica* L." and its by-products: A decade evidence of their health-promoting benefits towards the development of novel food formulations. *Trends in Food Science and Technology, 127*, 1–13. https://doi.org/10.1016/j.tifs.2022.06.010

Borderías, A. J., Tovar, C. A., Domínguez-Timón, F., Díaz, M. T., Pedrosa, M. M., & Moreno, H. M. (2020). Characterization of healthier mixed surimi gels obtained through partial substitution of myofibrillar proteins by pea protein isolates. *Food Hydrocolloids, 107*, Article 105976. https://doi.org/10.1016/j.foodhyd.2020.105976

Buamard, N., & Benjakul, S. (2015). Improvement of gel properties of sardine (*Sardinella albella*) surimi using coconut husk extracts. *Food Hydrocolloids, 51*, 146–155. https://doi.org/10.1016/j.foodhyd.2015.05.011

Buamard, N., Benjakul, S., & Konno, K. (2017). Improvement of gel quality of sardine surimi with low setting phenomenon by ethanolic coconut husk extract. *Journal of Texture Studies, 48*(1), 47–56. https://doi.org/10.1111/jtxs.12207

Buamard, N., Singh, P., Zhou, A., Ma, L., Zhang, B., & Benjakul, S. (2024). Ethanolic duea ching extract in combination with microbial transglutaminase: Strengthening effect on mince gel and cross-linking of myofibrillar proteins from Indian mackerel. *Journal of Agriculture and Food Research, 18*, Article 101459. https://doi.org/10.1016/j.jafr.2024.101459

Bukvički, D., Novaković, M., Ghani, N. B., Marin, P. D., & Asakawa, Y. (2018). Secondary metabolites from endemic species *Iris adriatica* Trinajstić ex Mitić (Iridaceae). *Natural Product Research, 32*, 1849–1852. https://doi.org/10.1080/14786419.2017.1402309

Cai, Q., Wu, Y., Li, L., Wang, Y., Yang, X., & Zhao, Y. (2017). Lipid oxidation and fatty acid composition in salt-dried yellow croaker (Pseudosciaena polyactis) during processing. *Journal of Ocean University of China, 16*(5), 855–862. https://doi.org/10.1007/s11802-017-3233-8

Cava, R., & Ladero, L. (2024). Using polyphenol-rich extracts from tropical fruit byproducts to control lipid and protein oxidation in cooked chicken models. *European Food Research and Technology, 250*(11), 2809–2820. https://doi.org/10.1007/s00217-024-04577-x

Cheng, J., Tang, D., Yang, H., Wang, X., Zhu, M., & Liu, X. (2021). The dose-dependent effects of polyphenols and malondialdehyde on the emulsifying and gel properties of myofibrillar protein-mulberry polyphenol complex. *Food Chemistry, 360*, Article 130005. https://doi.org/10.1016/j.foodchem.2021.130005

Dębczak, A., Grzegorczyk, A., Świątek, Ł., Sandomierski, M., Fekner, Z., Tyśkiewicz, K., & Milovanovic, S. (2024). Green and sustainable recovery of polyphenols, flavonoids, alkaloids, and pigments from green tea leaves: Comparative analysis of soxhlet, accelerated solvent, and supercritical fluid extraction techniques. *Sustainable Chemistry and Pharmacy, 42*, Article 101810. https://doi.org/10.1016/j.scp.2024.101810

De Carvalho, T. C. L., & Nunes, C. A. (2021). Smartphone-based method for the determination of chlorophyll and carotenoid contents in olive and avocado oils: An approach with calibration transfer. *Journal of Food Composition and Analysis, 104*, Article 104164. https://doi.org/10.1016/j.jfca.2021.104164

Ding, N., Sun, X., Yu, Q., Hong, H., Luo, Y., & Tan, Y. (2024). Unlocking the secrets of crude myofibril-bound serine protease from grass carp: The role in degrading myofibrillar proteins. *Food Chemistry, 437*, Article 137844. https://doi.org/10.1016/j.foodchem.2023.137844

Doğan Ulu, Ö., Ulu, A., Birhanlı, E., Pekdemir, M. E., & Ateş, B. (2026). Carboxymethyl chitosan/inulin composite films incorporated with different phenolic compounds as a potential new material for food packaging applications. *International Journal of Biological Macromolecules, 335*, Article 149344. https://doi.org/10.1016/j.ijbiomac.2025.149344

Du, L., & Betti, M. (2016). Chicken collagen hydrolysate cryoprotection of natural actomyosin: Mechanism studies during freeze-thaw cycles and simulated digestion. *Food Chemistry, 211*, 791–802. https://doi.org/10.1016/j.foodchem.2016.05.092

Duan, W., Qiu, H., Htwe, K. K., Wang, Z., Liu, Y., Wei, S., Xia, Q., Sun, Q., Han, Z., & Liu, S. (2023). Correlation between water characteristics and gel strength in the gel formation of golden pompano surimi induced by dense phase carbon dioxide. *Foods, 12*(5), 1090. https://doi.org/10.3390/foods12051090

Ebrahimi, P., Bayram, I., Lante, A., & Decker, E. A. (2024). Acid-hydrolyzed phenolic extract of parsley (*Petroselinum crispum* L.) leaves inhibits lipid oxidation in soybean oil-in-water emulsions. *Food Research International, 187*, Article 114452. https://doi.org/10.1016/j.foodres.2024.114452

Elhewehy, A. A., El-fishawy, A. M., El-Rashedy, A. A., Fayez, A. M., Fayed, M. A. A, & Mohsen, E. (2025). UPLC-ESI–MS/MS phytochemical profile, in vitro, in vivo, and in silico anti-Alzheimer's activity assessment of *pithecellobium dulce* (Roxb.) benth. Leaves. *Future Journal of Pharmaceutical Sciences, 11*, 30. https://doi.org/10.1186/s43094-025-00776-9

Fatan Tikmedash, B., Sahari, M. A., Barzegar, M., Ahmadi Gavlighi, H., & Asghari, M. (2026). Lupin protein as a sustainable alternative to conventional proteins in meat analogues produced via thermo-mechanical stretching. *LWT, 249*, Article 119386. https://doi.org/10.1016/j.lwt.2026.119386

Fathy, H. M., Abd El-Maksoud, A. A., Cheng, W., & Elshaghabee, F. M. F (2022). Value-added utilization of citrus peels in improving functional properties and probiotic viability of acidophilus-bifidus-thermophilus (ABT)-type synbiotic yoghurt during cold storage. *Foods, 11*(17), 2677. https://doi.org/10.3390/foods11172677

Gani, A., Benjakul, S., & Nuthong, P. (2018). Effect of virgin coconut oil on properties of surimi gel. *Journal of Food Science and Technology, 55*(2), 496–505. https://doi.org/10.1007/s13197-017-2958-0

Gier, H., Roth, W., Schumm, S., & Gerhards, M. (2002). Structures of 1,2,3-trihydroxybenzene in the S0 and S1 states. *Journal of Molecular Structure, 610*, 1–16. https://doi.org/10.1016/S0022-2860(01)00786-4

Han, G., & Li, Y. (2024). A review of inhibition mechanisms of surimi protein hydrolysis by different exogenous additives and their application in improving surimi gel quality. *Food Chemistry, 456*, Article 140002. https://doi.org/10.1016/j.foodchem.2024.140002

Han, M., Wang, P., Xu, X., & Zhou, G. (2014). Low-field NMR study of heat-induced gelation of pork myofibrillar proteins and its relationship with microstructural characteristics. *Food Research International, 62*, 1175–1182. https://doi.org/10.1016/j.foodres.2014.05.062

Han, X., Liang, Q., Rashid, A., Qayum, A., Rehman, A., Zhong, M., Sun, Y., Liu, Y., Ma, H., Miao, S., & Ren, X. (2024). The effects of different hydrocolloids on lotus root starch gelatinization and gels properties. *International Journal of Biological Macromolecules, 257*, Article 128562. https://doi.org/10.1016/j.ijbiomac.2023.128562

Kaur, P., Gupta, R. C., Dey, A., Malik, T., & Pandey, D. K. (2020). Validation and quantification of major biomarkers in 'Mahasudarshan Churna'- an ayurvedic polyherbal formulation through high-performance thin-layer chromatography. *BMC Complementary Medicine and Therapies, 20*(1), 184. https://doi.org/10.1186/s12906-020-02970-z

Latiff, N. A., Ong, P. Y., Abd Rashid, S. N. A., Abdullah, L. C., Mohd Amin, N. A., & Fauzi, N. A. M. (2021). Enhancing recovery of bioactive compounds from Cosmos caudatus leaves via ultrasonic extraction. *Scientific Reports, 11*(1), Article 17297. https://doi.org/10.1038/s41598-021-96623-x

Liu, J., Hefni, M. E., & Witthöft, C. M. (2021). Phenolic compounds in Swedish dried pulses: Characterization, retention and distribution during hydrothermal treatment processes. *Journal of Food Composition and Analysis, 102*, Article 104056. https://doi.org/10.1016/j.jfca.2021.104056

Liu, W., Gao, H., He, J., Yu, A., Sun, C., Xie, Y., Yao, H., Wang, H., Duan, Y., Hu, J., Tang, D., Ran, T., & Lei, Z. (2024). Effects of dietary *Allium mongolicum* Regel powder supplementation on the growth performance, meat quality, antioxidant capacity and muscle fibre characteristics of fattening Angus calves under heat stress conditions. *Food Chemistry, 453*, Article 139539. https://doi.org/10.1016/j.foodchem.2024.139539

Liu, X., Xie, Y., Ma, Y., Zhang, W., Zhou, K., Xu, Y., & Xu, B. (2026). Quality improvement of ready-to-eat chicken breast after two-stage heating: The role of actomyosin

dissociation. *Food Chemistry, 511*, Article 148814. https://doi.org/10.1016/j.foodchem.2026.148814
Ma, J., Liu, X., Wang, K., Jin, Y., & Liu, Y. (2024). New insight into yolk sphere microgel structure impacted by lipid and protein distribution changing under heating processing. *Food Chemistry, 435*, Article 137520. https://doi.org/10.1016/j.foodchem.2023.137520
Mittal, A., Singh, A., Zhang, B., Visessanguan, W., & Benjakul, S. (2022). Chitooligosaccharide conjugates prepared using several phenolic compounds via ascorbic acid/H2O2 free radical grafting: characteristics, antioxidant, antidiabetic, and antimicrobial activities. *Foods, 11*(7), 920. https://doi.org/10.3390/foods11070920
Mleko, S., & Foegeding, E. A. (2000). pH induced aggregation and weak gel formation of whey protein polymers. *Journal of Food Science, 65*(1), 139–143. https://doi.org/10.1111/j.1365-2621.2000.tb15969.x
Moshawih, S., Cheema, M. S., Ibraheem, Z. O., Tailan, N. D., & Hakim, M. N. (2017). Cosmos caudatus extract/fractions reduce smooth muscle cells migration and invasion in vitro: A potential benefit of suppressing atherosclerosis. *Porto Biomedical Journal, 2*(6), 293–300. https://doi.org/10.1016/j.pbj.2017.03.008
Murugesan, S., Buamard, N., Zhou, A., Zhao, Y., Zhang, B., & Benjakul, S. (2025). Improvement of gelling properties of surimi from threadfin bream (*Nemipterus* spp.) using saponin. *Applied Food Research, 5*(2), Article 101318. https://doi.org/10.1016/j.afres.2025.101318
Namal Senanayake, S. P. J. (2013). Green tea extract: Chemistry, antioxidant properties and food applications – A review. *Journal of Functional Foods, 5*(4), 1529–1541. https://doi.org/10.1016/j.jff.2013.08.011
Olatunde, O. O., Benjakul, S., & Vongkamjan, K. (2018). Antioxidant and antibacterial properties of guava leaf extracts as affected by solvents used for prior dechlorophyllization. *Journal of Food Biochemistry, 42*(5), Article e12600. https://doi.org/10.1111/jfbc.12600
Paixao, N., Perestrelo, R., Marques, J., & Camara, J. (2007). Relationship between antioxidant capacity and total phenolic content of red, rosé and white wines. *Food Chemistry, 105*(1), 204–214. https://doi.org/10.1016/j.foodchem.2007.04.017
Panpipat, W., Thongkam, P., Boonmalee, S., Çavdar, H. K., & Chaijan, M. (2023). Surimi Production from Tropical Mackerel: A simple washing strategy for better utilization of Dark-Fleshed Fish Resources. *Resources, 12*(10), 126. https://doi.org/10.3390/resources12100126
Park, M.-H., Ko, T.-Y., Ku, K.-M., Ran Do, K., Kang, S.-M., Lee, J., Eum, H.-L., Yoon, H. I., Choi, S.-H., Park, G. H., & Malka, S. K. (2026). Cultivar-dependent peel browning in oriental melon is associated with surface protection and stress response regulation during storage. *Postharvest Biology and Technology, 235*, Article 114228. https://doi.org/10.1016/j.postharvbio.2026.114228
Park, J. W. (2011). Code of practice for frozen Surimi. In J. Park (Ed.), *Surimi and surimi seafood* (2nd, pp. 520–527). CRC Press. https://doi.org/10.1016/j.fbp.2010.07.005.
Pati, B. K., Priyadarshini, M. B., Mehta, N. K., Patel, A. B., Gaurav, K., & Anand, S. (2026). Impact of quercetin on the functional and structural propertiesof chitooligosaccharide (CHOS)-enriched surimi. *Gels, 12*, 776. https://doi.org/10.3390/gels12090776
Pielesz, A., Biniaś, D., & Wieczorek, J. (2011). FT-IR spectroscopic analysis in monitoring of hydroxyl stretching vibrations in plant hydrogels. *Polimery w Medycynie, 41*(4), 33–42.
Qi, W., Qi, W., Xiong, D., & Long, M. (2022). Quercetin: Its antioxidant mechanism, antibacterial properties and potential application in prevention and control of toxipathy. *Molecules, 27*, 6545. https://doi.org/10.3390/molecules27196545
Raposo, F., Borja, R., & Gutiérrez-González, J. A. (2024). A comprehensive and critical review of the unstandardized Folin-Ciocalteu assay to determine the total content of polyphenols: The conundrum of the experimental factors and method validation. *Talanta, 272*, Article 125771. https://doi.org/10.1016/j.talanta.2024.125771
Raspe, D. T., da Silva, C., & Cláudio da Costa, S. (2022). Compounds from *Stevia rebaudiana* bertoni leaves: An overview of non-conventional extraction methods and challenges. *Food Bioscience, 46*, Article 101593. https://doi.org/10.1016/j.fbio.2022.101593
Rompas, J. J. I., Turagan, S. H., Gunawan, F. A., Rampengan, D. D. C. H., Seran, E. R., Nababan, S. P., Romano, R., Santini, A., & Nurkolis, F. (2025). Bee propolis-enhancing its nutraceutical and nutritional value through optimized extraction: An opinion focus on techniques and solvent effects. *Applied Food Research, 5*(2), Article 101538. https://doi.org/10.1016/j.afres.2025.101538
Sae-Leaw, T., Benjakul, S., & O'Brien, N. M (2016). Effect of pretreatments and defatting of seabass skins on properties and fishy odor of gelatin. *Journal of Food Biochemistry, 40*(6), 741–753. https://doi.org/10.1111/jfbc.12267
Sharma, S., Majumdar, R. K., & Mehta, N. K. (2025). Bioactive compounds from the mosambi (*Citrus limetta*) peel and their fortification into tilapia surimi improve gelling and textural properties. *Biomass Conversion and Biorefinery, 15*(4), 4955–4967. https://doi.org/10.1007/s13399-023-04142-8
Shen, R., Yang, X., Duan, Y., Liu, M., Zhang, L., He, L., Chen, C., Wang, W., Tong, L., & Han, G. (2025). Preparation of quercetin microcapsules with bovine serum albumin-arabinoxylan cold-set gels as wall material and its application in beef preservation. *Food Chemistry: X, 29*, Article 102714. https://doi.org/10.1016/j.fochx.2025.102714
Shi, H., Zhou, T., Wang, X., Zou, Y., Wang, D., & Xu, W. (2021). Effects of the structure and gel properties of myofibrillar protein on chicken breast quality treated with ultrasound-assisted potassium alginate. *Food Chemistry, 358*, Article 129873. https://doi.org/10.1016/j.foodchem.2021.129873
Si, S., Huang, D., Wang, T., Sun, Y., Qian, Y., & Liu, X. (2025). Gelation mechanism analysis of low-salt silver carp (*Hypophthalmichthys molitrix*) surimi enhancing by ultrasonication combined apple pectin, citrus pectin, or peach gum. *Food Chemistry: X, 31*, Article 103175. https://doi.org/10.1016/j.fochx.2025.103175
Singh, S., Chidrawar, V. R., Hermawan, D., Nwabor, O. F., Olatunde, O. O., Jayeoye, T. J., Samee, W., Ontong, J. C., & Chittasupho, C. (2023). Solvent-assisted dechlorophyllization of *Psidium guajava* leaf extract: Effects on the polyphenol content, cytocompatibility, antibacterial, anti-inflammatory, and anticancer activities. *South African Journal of Botany, 158*, 166–179. https://doi.org/10.1016/j.sajb.2023.04.029
Sinlapapanya, P., Sumpavapol, P., Aluko, R. E., Nuthong, P., Zhang, B., & Benjakul, S. (2023). Antioxidant and antibacterial activities of indigenous plant leaf ethanolic extracts and their use for extending the shelf-life of Nile tilapia (*Oreochromis niloticus*) mince. *International Journal of Food Science & Technology, 58*(4), 1987–1998. https://doi.org/10.1111/ijfs.16358
Tagrida, M., & Benjakul, S. (2020). Ethanolic extract of Betel (*Piper betle* L.) and Chaphlu (*Piper sarmentosum* Roxb.) dechlorophyllized using sedimentation process: Production, characteristics, and antioxidant activities. *Journal of Food Biochemistry, 44*(12). https://doi.org/10.1111/jfbc.13508
Tagrida, M., & Benjakul, S. (2021). Betel (*Piper betle* L.) leaf ethanolic extracts dechlorophyllized using different methods: Antioxidant and antibacterial activities, and application for shelf-life extension of Nile tilapia (*Oreochromis niloticus*) fillets. *RSC Advances, 11*(29), 17630–17641. https://doi.org/10.1039/D1RA02464G
Tsuchiya, Y., Hirono, Y., & Sonobe, R. (2025). Estimating chlorophyll content in tea leaves using spectral reflectance and deep learning methods. *Ecological Informatics, 91*, Article 103399. https://doi.org/10.1016/j.ecoinf.2025.103399
Wei, W., Hu, W., Zhang, X. Y., Zhang, F. P., Sun, S. Q., Liu, Y., & Xu, C. H. (2018). Analysis of protein structure changes and quality regulation of surimi during gelation based on infrared spectroscopy and microscopic imaging. *Scientific Reports, 8*(1), 5566. https://doi.org/10.1038/s41598-018-23645-3
Wu, J., Li, C., Li, L., Yang, X., Wang, Y., & Zhou, W. (2022). Improved physicochemical properties and product characteristics of tilapia surimi by tea polyphenols during chilled storage. *LWT, 167*, Article 113822. https://doi.org/10.1016/j.lwt.2022.113822
Wu, Z., Qu, Y., Li, O., Benjakul, S., & Zhou, A. (2025). Improvement of gel properties of *Nemipterus virgatus* myofibrillar protein emulsion gels by curdlan: Development and application to emulsified surimi. *Gels, 11*(9), 753. https://doi.org/10.3390/gels11090753
Xie, D., Tang, Y., & Dong, G. (2024). Various factors affecting the gel properties of surimi: A review. *Journal of Texture Studies, 55*(3). https://doi.org/10.1111/jtxs.12847
Yang, R., Juma, N. S., Zhao, Y., Zheng, B., Xu, Y., Gao, Y., Jia, R., Gao, P., & He, Y. (2025). Factors influencing surimi gelling properties and natural additive–based gel fortification strategies: A review. *Comprehensive Reviews in Food Science and Food Safety, 24*(1). https://doi.org/10.1111/1541-4337.70067
Zhang, H., Xiong, Y., Bakry, A. M., Xiong, S., Yin, T., Zhang, B., Huang, J., Liu, Z., & Huang, Q. (2019). Effect of yeast β-glucan on gel properties, spatial structure and sensory characteristics of silver carp surimi. *Food Hydrocolloids, 88*, 256–264. https://doi.org/10.1016/j.foodhyd.2018.10.010